Table II. Final Characterization of [CoCo] and [CoCu]

		g_1	g_2	g_3	J^a (K)	$\lvert j\rvert^a$ (K)	$\alpha = J_\perp/J_\parallel$
	$(Co)_h{}^b$	5.90	3.88		−6.3	<0.05	0.22
[CoCo]	$(Co)_q$	10.1	1.43	1.24			
[CoCu]	$(Cu)_q$	2.27	2.02		−2.7	<0.05	0.35

[a] Scaling factors have been introduced to account for the effective spin of Co(II) (these factors are 9/25 for [CoCo] and 3/5 for [CoCu]. [b] h and q refer to the "hydrated" and "chelated" sites, respectively.

respect to the principal magnetic axes.

Considering both the alternation of the Landē factors and the alternating character of the exchange coupling, we have derived the exact solutions for the spin-1/2 Ising chain and compared the results to the experiment. Although the analysis of the above systems is not straightforward, a reasonable agreement between the parameters determined from different (and complementary) experiments was obtained. Thus, the magnetic susceptibility data appeared to be very useful to emphasize the strong dimerization of the chains ($j/J < 0.05$). Conversely, due to the large number of adjustable parameters used in the magnetic analysis, it results in a large uncertainty in their absolute values.

In turn, the specific heat results have shown to be relatively insensitive to the dimensionality of these systems. Thus, the Schottky anomaly can be well-explained in terms of (alternating) Ising chains or by assuming anisotropic exchange coupled dimers. In view of the magnetic susceptibility analysis, the second model seems to be the more realistic. Finally, due to the limited number of parameters in the specific heat analysis, we obtain reliable values for J and α.

Hence, from the above results and the EPR findings, we have a satisfying characterization of both compounds (Table II).

The strong difference between J and j observed in both cases cannot be explained by simple structural arguments (metal–metal distances or bond angles of bridging ligands, for instance). In turn, by focusing on the zigzag chain structure, and the directions of anisotropy for the Ising-type ions, it is likely that quantum effects do induce a significant alternation in the exchange coupling. In this respect, a rigorous analysis of the exchange mechanisms accounting for the above effects and the available overlap between metallic magnetic orbitals (via bridging atoms) is not straightforward in the present case.

Finally, in regards to the interchain interactions, it is worth noticing that their influence is negligible in both systems (no λ-type anomaly in the specific heat data), while they are quite prominent in the related systems [MnCo], [MnNi], and [MnCu]. The manifestation of such interactions is obviously closely related to the ground spin configuration of the chain. Thus, drastic effects are anticipated for 1d ferrimagnets with two distinct spins (high spin ground state), but, conversely, the effect will be of the second order when only g factors alternate (the ground configuration is $S = 0$). This warrants the description of [CoCo] and [CoCu] in terms of well-isolated dimerized chains.

Acknowledgment. This work was supported in part by the European Economic Community (Grant ST2/164) and the Comision Asesora de Investigaciones Cientificas y Tecnicas (2930/83). One of us (E.C.) has also obtained a grant from Generalitat Valenciana.

Registry No. [CoCo], 84222-22-0; [CoCu], 84222-24-2.

Metal-Assisted Three-Fragment Demolition of the Dithiocarbonate Ligand: A New Synthetic Route to Homo- and Heterobinuclear Bis(μ-sulfido)metal Complexes. Chemical, Electrochemical, and Spectroscopic Characterization of a Family of Complexes of Iron, Cobalt, Rhodium, and Platinum with Bridging Sulfido Ligands

Claudio Bianchini,*† Andrea Meli,† Franco Laschi,‡ Alberto Vacca,† and Piero Zanello‡

Contribution from the Istituto per lo Studio della Stereochimica ed Energetica dei Composti di Coordinazione, CNR, Via J. Nardi 39, 50132 Firenze, and Dipartimento di Chimica, Università di Siena, Pian dei Mantellini, Siena, Italy. *Received September 22, 1987*

Abstract: Homo- and heterobinuclear bis(μ-sulfido) complexes of the general formula $[(triphos)Rh(\mu\text{-}S)_2M(L)](BPh_4)_x$ [M = Rh, L = triphos, $x = 2$; M = Co, L = triphos, $x = 1, 2$; M = Pt, L = diphos, $x = 1$; M = Fe, L = etriphos and CO, $x = 1$] [triphos = $MeC(CH_2PPh_2)_3$; diphos = $Ph_2PCH_2CH_2PPh_2$; etriphos = $MeC(CH_2PEt_3)_2$] are obtained by reaction of the dithiocarbonates $[(triphos)Rh(S_2CO)]BPh_4$ or $(triphos)Co(S_2CO)$ with coordinatively unsaturated fragments. The reactions proceed through chelotropic elimination of carbon monoxide from the RhSCOS or CoSCOS cycles promoted by interaction of the externally added metal fragment with the two sulfur atoms of the dithiocarbonate ligands. The electrochemical behavior in CH_2Cl_2 solution of all of the bis(μ-sulfido) dimers has been investigated. In particular, the complexes containing the $Rh(\mu\text{-}S)_2Rh$, $Rh(\mu\text{-}S)_2Co$, and $Co(\mu\text{-}S)_2Co$ cores undergo electron-transfer reactions that encompass the 0, 1+, and 2+ charges with no change of the primary geometry. By contrast, the compounds with the $Rh(\mu\text{-}S)_2Fe$ and $Rh(\mu\text{-}S)_2Pt$ cores rapidly decompose on addition of electrons. Chemical and electrochemical techniques have been used to prepare the paramagnetic congeners $[(triphos)Rh(\mu\text{-}S)_2Rh(triphos)]BPh_4$ and $[(triphos)Rh(\mu\text{-}S)_2Co(triphos)]BPh_4$. The products have been characterized by IR, ^{31}P NMR, and ESR spectroscopies. The reactions of the compounds with molecular hydrogen have been investigated.

Binuclear complexes with sulfido bridges are of current interest, owing to their use as models for biological systems,[1] as well as the variety of their application in stoichiometric[2] and catalytic reactions.[2i] Also, a great number of sulfido-bridged dimers display extensive electron-transfer chemistry, which does not destroy the

† CNR.
‡ Università di Siena.

(1) Berg, J. M.; Holm, R. H. In *Metal Ions in Biology*; Spiro, T. G., Ed.; Wiley-Interscience: New York, 1982; Vol. 4, Chapter 1.

0002-7863/88/1510-3913$01.50/0

Scheme I

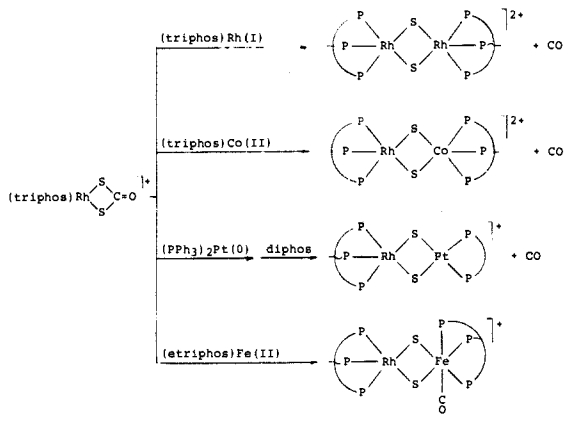

complex framework.[2d-e,3] Such a property makes these compounds potential redox catalysts.[4]

Whereas a large number of synthetic methods have been developed to prepare homobinuclear μ-S complexes of transition metals, very few routes to mixed-metal derivatives are still available.[5]

We report here a new, clean, and largely utilizable method to synthesize homo- and heterobimetallic bis(μ-sulfido) complexes of rhodium, iron, cobalt, and platinum with phosphine ligands. The heterobinuclear derivatives are of particular importance because of the present interest in the chemistry of compounds with metal sites of different nature.

Our interest in the chemistry of bridging sulfido complexes stems from their potential catalytic use in homogeneous hydrogenations.[2i] In this respect, we have recently reported the double addition of H_2 to the disulfur-bridged dimeric cation of rhodium(III), $[(triphos)Rh(\mu\text{-}S)_2Rh(triphos)]^{2+}$ [eq 1; triphos = $MeC(CH_2PPh_2)_3$].[6] In an effort to understand the underlying

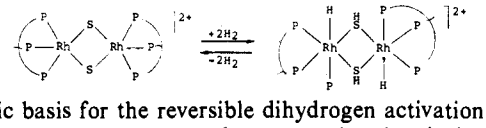

(1)

electronic basis for the reversible dihydrogen activation shown in eq 1, we now compare and contrast the chemical, electrochemical, and spectroscopic properties of $[(triphos)Rh(\mu\text{-}S)_2Rh(triphos)]^{2+}$ with those of the homo- and heterobinuclear congeners $[(triphos)Co(\mu\text{-}S)_2Co(triphos)]^{2+}$ and $[(triphos)Rh(\mu\text{-}S)_2Co(triphos)]^{2+}$. The results point out the importance of both the nature and the oxidation state of the metals in affecting the reactivity toward H_2.

Results

Synthesis and Characterization of the Compounds. Scheme I describes the syntheses of the complex cations contained in

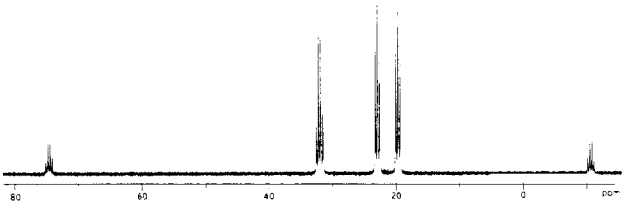

Figure 1. $^{31}P\{^1H\}$ NMR (acetone, 298 K, 32.19 MHz) of $[(triphos)Rh(\mu\text{-}S)_2Pt(diphos)]BPh_4$ (H_3PO_4 reference).

$[(triphos)Rh(\mu\text{-}S)_2Rh(triphos)](BPh_4)_2$ (**1**), $[(triphos)Rh(\mu\text{-}S)_2Co(triphos)](BPh_4)_2$ (**2**), $[(triphos)Rh(\mu\text{-}S)_2Pt(diphos)]BPh_4$ (**3**), and $[(triphos)Rh(\mu\text{-}S)_2Fe(CO)(etriphos)]BPh_4$ (**4**) [diphos = $Ph_2PCH_2CH_2PPh_2$; etriphos = $MeC(CH_2PEt_2)_3$]. In a typical procedure, a solution of the dithiocarbonate complex $[(triphos)Rh(S_2CO)]BPh_4$ (**5**)[7] is added to a solution of the appropriate metal fragment at room temperature. In most instances, the reactions are complete within the time of mixing of the coreactants, and the products are precipitated by addition of $NaBPh_4$. With the exception of the Rh/Fe compound, carbon monoxide is evolved and detected by GC. All of the compounds **1–4** are crystalline, diamagnetic solids, air-stable in the solid state and in deoxygenated solutions in which they behave as 1:2 (**1**/**2**) or 1:1 (**3**/**4**) electrolytes. The IR spectra are unexceptional as compared to those of dimeric triphos complexes with halide bridges[8] and that of the Rh/Fe dimer, which contains a strong band at 1950 cm^{-1}, indicating the presence of a terminal carbonyl group. A further absorption at 1030 cm^{-1} is assigned to C–CH_3 rocking of the ethyl substituents on the phosphorus atoms of etriphos.[9] A useful diagnostic tool used to define the solution-state stereochemistry of the complexes is represented by $^{31}P\{^1H\}$ NMR spectroscopy. The six terminal phosphorus atoms in **1** are not distinguishable in the temperature range 303–213 K, since they give rise in DMF to a unique resonance at 23.92 ppm split by the rhodium nuclei into a doublet ($J_{P\text{-}Rh}$ = 101.8 Hz). Such a situation is well established and attributed to the absence of any rotational barrier about the axis that connects the two metals,[10] each of which may be imagined as belonging to a five-coordinate species of the type $[(triphos)RhX_2]$ (X = monofunctional ligand). Complexes of the latter type are generally fluxional at ambient temperatures, the exchange of the phosphorus atoms occurring through an intramolecular non-bond-breaking isomerization between square-planar and trigonal-bipyramidal conformations.[7,10,11] Extended Hückel calculations have shown that these two geometries are very close in energy,[10] in nice agreement with the fact that the stereochemical rigidity of five-coordinate triphos complexes on the NMR time scale is generally observed at very low temperatures.[11]

At variance with **1**, the two triphosphine ligands in the ^{31}P NMR spectrum (acetone, 293 K) of the isoelectronic derivative **2** are distinguishable because they are liniked to different metals. No coupling between the phosphorus atoms of the two triphos ligands is observed: A doublet centered at 11.67 ppm ($J_{P\text{-}Rh}$ = 131 Hz) and a singlet at 32.23 ppm are easily assigned to the ligands on rhodium and cobalt, respectively. By contrast, a rather strong coupling ($J_{P_{triphos}\text{-}P_{diphos}}$ = 11 Hz) between the two equivalent phosphorus atoms of diphos and the three of triphos is found for the Rh/Pt dimer **3** whose spectrum is shown in Figure 1. As expected, the triphos ligand originates a doublet of triplets centered at 21.60 ppm ($J_{P\text{-}Rh}$ = 106.4 Hz) while the resonance of diphos consists of a quartet at 32.54 ppm ($J_{P\text{-}Pt}$ = 2809 Hz).

Although still exhibiting a first-order ^{31}P NMR pattern, constant in the temperature range 298–203 K, the spectrum of the

(2) (a) Seyferth, D.; Kiwan, A. M. *J. Organomet. Chem.* **1985**, *286*, 219. (b) Hofler, M.; Baitz, A. *Chem. Ber.* **1976**, *109*, 3147. (c) Herberhold, M.; Jellen, W.; Murray, H. H. *J. Organomet. Chem.* **1984**, *270* 65. (d) Casewith, C. J.; Haltiwanger, R. C.; Noordik, J.; Rakowski DuBois, M. *Organometallics* **1985**, *4*, 119. (e) Rajan, O. A.; McKenna, M.; Noordik, J.; Haltiwanger, R. C.; Rakowski DuBois, M. *Organometallics* **1984**, *3*, 831. (f) Kubas, G. J.; Wasserman, H. J.; Ryan, R. R. *Organometallics* **1985**, *4*, 419. (g) McKenna, M.; Wright, L. L.; Miller, D. J.; Tanner, L.; Haltiwanger, R. C.; Rakowski DuBois, M. *J. Am. Chem. Soc.* **1983**, *105*, 5329. (h) Briant, C. E.; Hor, T. S. A.; Howells, N. D.; Mingos, D. M. P. *J. Chem. Soc., Chem. Commun.* **1983**, 1118. (i) Rakowski DuBois, M. *J. Am. Chem. Soc.* **1983**, *105*, 3710.

(3) (a) Mayerle, J. J.; Denmark, E. E.; DePamphilis, B. V.; Ibers, J. A. *J. Am. Chem.* **1975**, *97*, 1032. (b) Cambray, J.; Lane, R. W.; Wedd, A. G.; Johnson, R. W.; Holm, R. H. *Inorg. Chem.* **1977**, *16*, 2565. (c) Wong, G. B.; Bobrik, M. A.; Holm, R. H. *Ibid.* **1978**, *17*, 578. (d) Kubas, G. J.; Vergamini, P. J. *Ibid.* **1981**, *20*, 2667. (e) Hagen, K. S.; Watson, A. D.; Holm, R. H. *J. Am. Chem. Soc.* **1983**, *105*, 3905.

(4) Teruka, M.; Yajima, T.; Tsuchiya, A.; Matsumoto, Y.; Uchida, Y.; Hidai, M. *J. Am. Chem. Soc.* **1982**, *104*, 6834.

(5) (a) Coucouvanis, D.; Simbon, E. D.; Swenson, D.; Baenziger, N. C. *J. Chem. Soc., Chem. Commun.* **1979**, 361. (b) Coucouvanis, D.; Baeziger, N. C.; Simhon, E. D.; Stremple, D.; Swenson, D.; Kostikas, A.; Simopoulos, A.; Petrouleas, V.; Pepaefthymiou, V. *J. Am. Chem. Soc.* **1980**, *102*, 1730.

(6) Bianchini, C.; Mealli, C.; Meli, A.; Sabat, M. *Inorg. Chem.* **1986**, *25*, 4618.

(7) Bianchini, C.; Mealli, C.; Meli, A.; Sabat, M. *J. Chem. Soc., Chem. Commun.* **1985**, 1024.

(8) Sacconi, L.; Mani, F. *Transition Met. Chem. (N.Y.)* **1982**, *8*, 179.

(9) Bianchini, C.; Dapporto, P.; Mealli, C.; Meli, A. *Inorg. Chem.* **1982**, *21*, 612.

(10) Bianchini, C.; Mealli, C.; Meli, A.; Sabat, M.; Zanello, P. *J. Am. Chem. Soc.* **1987**, *109*, 185.

(11) Dahlemburg, L.; Mirzaei, F. *Inorg. Chim. Acta* **1985**, *97*, L1.

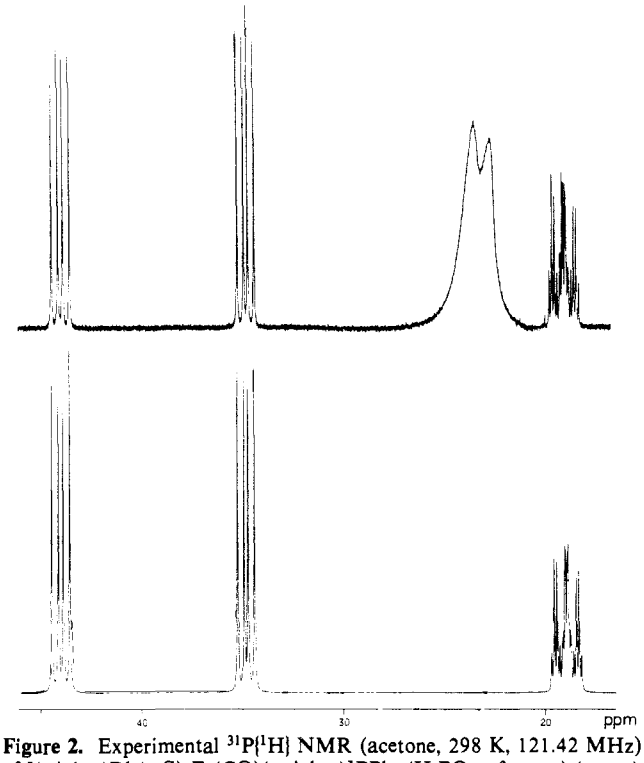

Figure 2. Experimental $^{31}P\{^1H\}$ NMR (acetone, 298 K, 121.42 MHz) of [(triphos)Rh(μ-S)$_2$Fe(CO)(etriphos)]BPh$_4$ (H_3PO_4 reference) (upper) and computed spectrum for the ABC spin system relative to the Fe-(etriphos) fragment (lower).

Rh/Fe dimer **4**, which is shown in Figure 2 together with the computed one,[12] is much more complicated than the previous ones. The triphos ligand that coordinates the rhodium atom gives rise to a broad doublet at 23.33 ppm (J_{P-Rh} = 101.6 Hz). The resonance of the etriphos ligand, which occupies three facial sites of an octahedron (see Scheme I), consists of an ABC spin system. One of the phosphorus nuclei is coupled also with the three phosphorus atoms of triphos, thus forming four quartets. The chemical shifts and the coupling constants are as follows: δ_{PA} 43.98, δ_{PB} 34.80, δ_{PC} 18.93; J_{PA-PB} = 39.27 Hz, J_{PA-PC} = 69.02 Hz, J_{PB-PC} = 63.17 Hz, $J_{PC-P_{triphos}}$ = 15.95 Hz (eq 2).

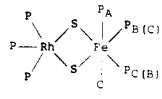

(2)

In spite of several theoretical and experimental studies, a clear-cut explanation of why only one of the two equatorial phosphorus nuclei of etriphos couples with triphos cannot be presently offered. Tentatively, this phenomenon may be attributed either to different bonding modes of the two sulfido groups in connecting ML_3 and ML_4 metal fragments or to a remarkable departure from the octahedron of the Fe(CO)(etriphos) fragment. Both hypotheses are substantiated by the ^{31}P NMR spin system exhibited by etriphos instead of the expected octahedral AB_2 one. In any case, the coupling of one phosphorus atom of etriphos with the three of triphos is well established as demonstrated by phosphorus decoupling experiments. In fact, irradiation of the rightmost resonance makes the line width at half-height of the triphos resonance sharpen to the value observed in compounds **1** and **2**.

Interestingly, the metal-promoted elimination of carbon monoxide from the η^2-*S*,*S*-dithiocarbonate ligand seems not to be a unique chemical property of **5**. In fact, we have also found that the Co(II) dithiocarbonate (triphos)Co(S_2CO) (**6**)[13] reacts with

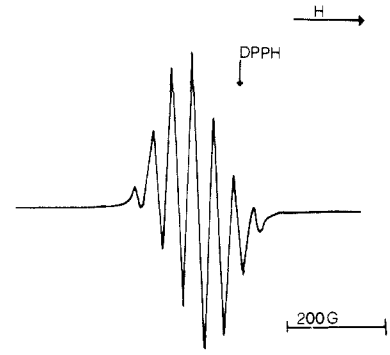

Figure 3. X-Band ESR spectrum of [(triphos)Rh(μ-S)$_2$Rh(triphos)]BPh$_4$ in CH_2Cl_2 solution at 298 K.

the (triphos)Rh^I fragment under the same conditions employed for **5** to give CO and a bis(μ-sulfido) dimer, namely [(triphos)-Rh(μ-S)$_2$Co(triphos)]BPh$_4$ (**7**) (eq 3).

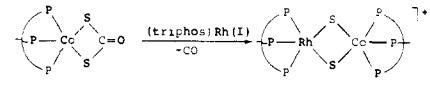

(3)

Compound **7**, which can be obtained either by reduction of **2** in CH_2Cl_2 with $NaBH_4$ in ethanol (eq 4) or by controlled-potential electrolysis (vide infra), is paramagnetic, with a magnetic moment corresponding to one unpaired spin (μ_{eff} 1.98 μ_B). The electronic

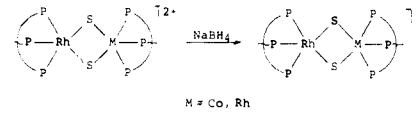

(4)

spectrum exhibits bands at 6900, 13 300, and 18 200 (sh) cm^{-1}. The compound is air stable neither in the solid state nor in solution, being rapidly oxidized to the dicationic derivative **2**. In deoxygenated solutions, **7** behaves as a 1:1 electrolyte.

Similar chemical and magnetic properties (μ_{eff} 1.70 μ_B) are exhibited by the complex [(triphos)Rh(μ-S)$_2$Rh(triphos)]BPh$_4$ (**8**), which is prepared either by treatment of **1** in CH_2Cl_2 with $NaBH_4$ in ethanol (eq 4) or by electrochemical reduction. The electronic spectrum shows absorption maxima at 6800, 11 000, and 19 000 (sh) cm^{-1}.

The X-band ESR spectrum of **8** in CH_2Cl_2 at 298 K (Figure 3) shows a septuplet ($\langle g \rangle$ = 2.06) consistent with coupling of one unpaired electron with six equivalent phosphorus nuclei, which indicates that the fluxional behavior of the monocationic derivative is essentially similar to that of the dimagnetic parent compound **1**. The total line width ΔH_{total} is 232.4 G while the hyperfine coupling constant ($\langle A_P \rangle$ = 39.6 G) is consistent with a strong interaction of the electron with the phosphorus nuclei.[14] The line shape of the spectrum does not put in evidence any additional hyperfine structure, as expected on account of the generally small coupling constants (c.a. 10 G)[14,15] of the electron with the rhodium nucleus ($I = {}^1/_2$). In this respect, notice that the line width of the seven absorptions is relatively large, the narrowest one being 21.6 G.

The frozen-solution spectrum (100 K; Figure 4; ΔH_{total} = 261.3 G) can be interpreted by using an $S = {}^1/_2$ spin Hamiltonian with g_1 = 2.149, g_2 = 2.066, and g_3 = 1.980. The three *g* values indicate noticeable anisotropy in the **g** tensor, typical of an "orthorhombic-type" spatial structure of **8**.

The X-band ESR spectrum of the heterobimetallic complex **7** in CH_2Cl_2 at 298 K consists of a broad signal (ΔH_{total} = 112.0 G) with no hyperfine structure ($\langle g \rangle$ = 2.106). The frozen-solution spectrum (100 K; Figure 5) is characterized by a partially resolved hyperfine structure with ΔH_{total} = 309.5 G and $\langle g \rangle$ = 2.099 (evaluated from the peak-to-peak distance). As is evident from

(12) The spectrum has been simulated by the Computer Program DAVINS (*J. Magn. Reson.* **1980**, *37*, 395; *Ibid.* **1980**, *37*, 409) adapted to the Gould Computer 32/27 by A. Vacca.

(13) Bianchini, C.; Meli, A.; Orlandini, A. *Inorg. Chem.* **1982**, *21*, 4166.

(14) Pilloni, G.; Zotti, G.; Zecchin, S. *J. Organomet. Chem.* **1986**, *317*, 357.

(15) Felthouse, T. R. *Prog. Inorg. Chem.* **1982**, *29*, 73.

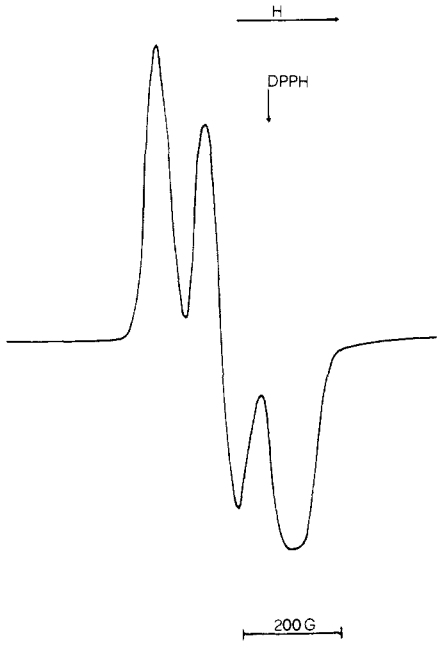

Figure 4. X-Band ESR spectrum of $[(triphos)Rh(\mu\text{-}S)_2Rh(triphos)]BPh_4$ in CH_2Cl_2 frozen solution (100 K).

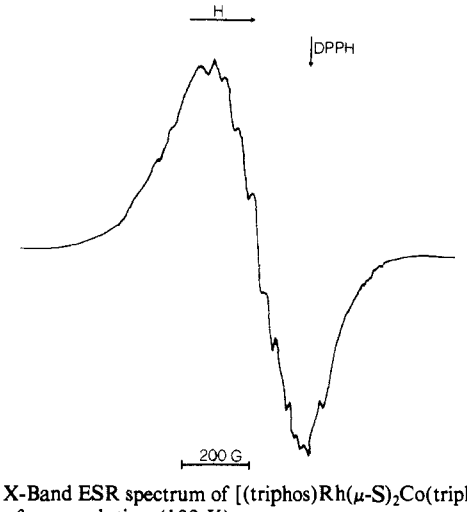

Figure 5. X-Band ESR spectrum of $[(triphos)Rh(\mu\text{-}S)_2Co(triphos)]BPh_4$ in CH_2Cl_2 frozen solution (100 K).

Figure 5, it is extremely difficult to identify the various components that originate the spectrum, i.e. the interactions of the electron with the cobalt ($I = {}^7/_2$), rhodium ($I = {}^1/_2$), and six phosphorus nuclei ($I = {}^1/_2$). However, it is worth noticing that replacement of cobalt for rhodium in the complex framework introduces a remarkable perturbation in the delocalization of the unpaired electron and causes complete loss of resolution of the g anisotropy and hyperfine components.

Attempts to synthesize a $(\mu\text{-}S)_2$ dimer containing rhodium and nickel were unsuccessful. Undoubtedly, the reaction of **5** with the $(triphos)Ni^{II}$ fragment is not a straightforward one. The mixture assumes various colors at different times of the reaction, indicating evolution of the species that are progressively formed. The final color is green, and green crystals of the μ-S homonuclear dimer $[(triphos)Ni(\mu\text{-}S)Ni(triphos)](BPh_4)_2$ (**9**)[16] are obtained in low yield (eq 5).

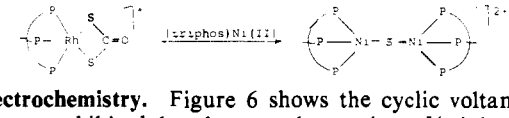

(5)

Electrochemistry. Figure 6 shows the cyclic voltammetric responses exhibited by the complex cations $[(triphos)Rh(\mu\text{-}S)_2M'(triphos)]^{2+}$ (M' = Rh, Co) as well as the homobinuclear derivative $[(triphos)Co(\mu\text{-}S)_2Co(triphos)]^{2+}$[17] in deaerated CH_2Cl_2 solutions.

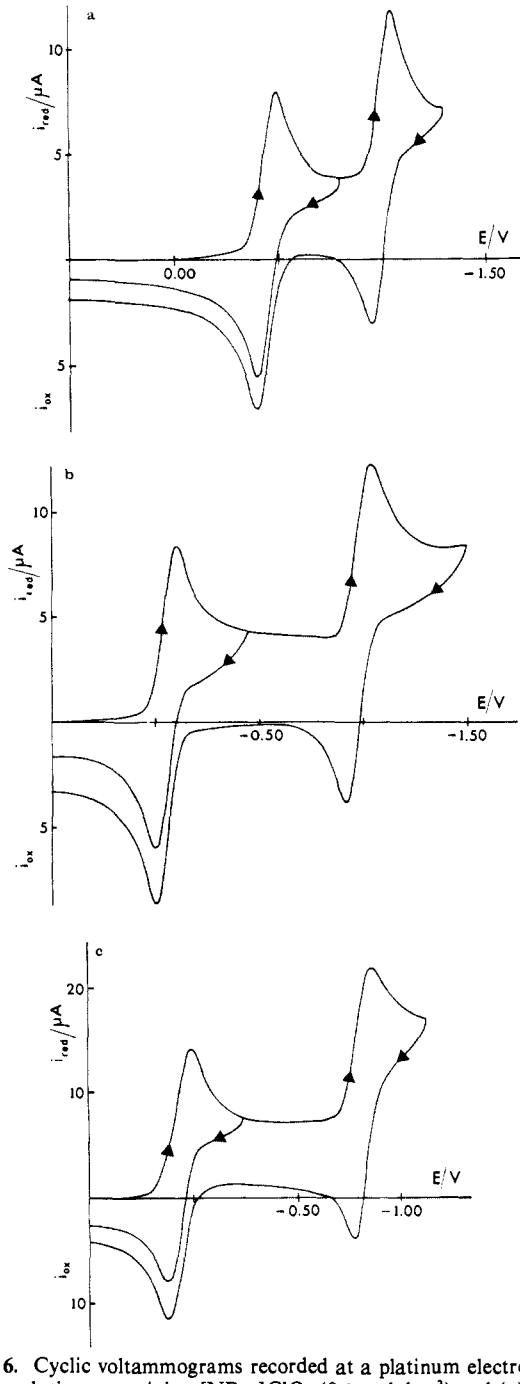

Figure 6. Cyclic voltammograms recorded at a platinum electrode on CH_2Cl_2 solutions containing $[NBu_4]ClO_4$ (0.1 mol dm^{-3}) and (a) $[(triphos)Rh(\mu\text{-}S)_2Rh(triphos)](BPh_4)_2$ (4.9×10^{-4} mol dm^{-3}), (b) $[(triphos)Rh(\mu\text{-}S)_2Co(triphos)](BPh_4)_2$ (5.5×10^{-4} mol dm^{-3}), and (c) $[(triphos)Co(\mu\text{-}S)_2Co(triphos)](BPh_4)_2$ (9.0×10^{-4} mol dm^{-3}). Scan rate 0.2 V s^{-1}.

Invariably, two subsequent cathodic processes are displayed, each of which showing a directly associated peak in the reverse scan. For the three cations, controlled-potential coulometric tests carried out in correspondence of the first reduction process showed the consumption of one electron/molecule. Cyclic voltammetry performed at the end of the electrolysis indicated that the electrogenerated species $[(triphos)M(\mu\text{-}S)_2M'(triphos)]^+$ (M, M' = Rh, Co) are quite stable, in nice agreement with their synthesis through chemical methods.

(16) Mealli, C.; Midollini, S.; Sacconi, L. *Inorg. Chem.* **1978**, *17*, 632.

(17) Ghilardi, C. A.; Mealli, C.; Midollini, S.; Nefedov, V. I.; Orlandini, A.; Sacconi, L. *Inorg. Chem.* **1980**, *19*, 2454.

Table I. Standard Electrode Potentials (V) for the Reduction Processes of the Dimers $[(Triphos)M(\mu\text{-}S)_2M'(triphos)]^{2+}$ (M, M' = Rh, Co) in Dichloromethane Solvent

dimer	$E°'(2+/1+)$	$E°'(1+/0)$
$[Rh/Rh]^{2+}$	−0.45	−1.00
$[Rh/Co]^{2+}$	−0.06	−0.98
$[Co/Co]^{2+}$	+0.07	−0.82

The analysis of the cyclic voltammetric responses exhibited by the $[Rh/Rh]^{2+}$ species with scan rates varying from 0.02 to 50 V s^{-1} revealed the following features. As far as the first cathodic process is concerned, the values of the parameters i_{pa}/i_{pc} (constantly equal to 1), $i_{pc}v^{-1/2}$ (constant), and ΔE_p (gradually increasing from 70 to 340 mV) are diagnostic of an uncomplicated one-electron reduction with a slight departure from the electrochemical reversibility, probably due to uncompensated solution resistances. The same trend holds with regards to the second cathodic process. However, controlled-potential electrolysis reveals that, under the present experimental conditions, the uncharged species $[(triphos)Rh(\mu\text{-}S)_2Rh(triphos)]$ is stable only for relatively short times. In fact, after the consumption of two electrons/molecule does the cyclic voltammogram clearly show its presence, but the electrolysis current does not stop and slowly continues up to the consumption of five electrons/molecule. At this stage, there is no more evidence in cyclic voltammetry for the presence of congeners of the parent dimer.

Qualitatively similar results are observed for the other complex cations. However, since $[(triphos)Co(\mu\text{-}S)_2Co(triphos)]$ has been isolated and X-ray authenticated,[17] its precipitation from the reaction mixture evidently blocks up the slow decomposition occurring in solution. Table I summarizes the redox potentials of the two subsequent one-electron cathodic processes within the series $[(triphos)M(\mu\text{-}S)_2M'(triphos)]^{2+}$ (M, M' = Rh; M, M' = Rh, Co; M, M' = Co/Co). The two consecutive charge transfers formally correspond to the metal-centered sequence

$$M(III)/M'(III) \underset{-e^-}{\overset{+e^-}{\rightleftharpoons}} M(III)/M'(II) \underset{-e^-}{\overset{+e^-}{\rightleftharpoons}} M(II)/M'(II)$$

The separation between the redox potentials of the two steps allows us to compute, according to a well-known treatment,[18] the comproportionation constant, K_{com}, for the equilibrium

$$M(III)/M'(III) + M(II)/M'(II) \rightleftarrows 2M(III)/M'(II)$$

In nice agreement with the ESR data, these K_{com} values (2×10^9, 3×10^{15}, and 5×10^{12} for the Rh/Rh, Rh/Co, and Co/Co species, respectively) indicate[19-21] that the mixed-valence dimers $[(triphos)M(\mu\text{-}S)_2M^{\bullet}(triphos)]^+$ may belong to the "class III" Robin–Day derivatives; i.e., the unpaired electron is completely delocalized around the metal–metal moiety.[22,23]

The electrochemical studies point out that it is possible to add or remove valence electrons both chemically and electrochemically with no consequential change of the primary geometry of the complexes. This means that the coordination polyhedron as well as the coordination number about each metal atom remain unchanged when electrons are added or removed. What changes is the charge of the whole complex, as is natural, and the so-called secondary geometry, i.e. the bond lengths in the coordination spheres of the metals.[17] In particular, the metal–metal distance gradually should increase on successive reductions as experimentally found for the two complexes $[(triphos)Co(\mu\text{-}S)_2Co(triphos)]^+$ and $[(triphos)Co(\mu\text{-}S)_2Co(triphos)]$ in which the Co–Co distances are 3.434 (8) and 3.597 (2) Å, respectively.[17]

Scheme II

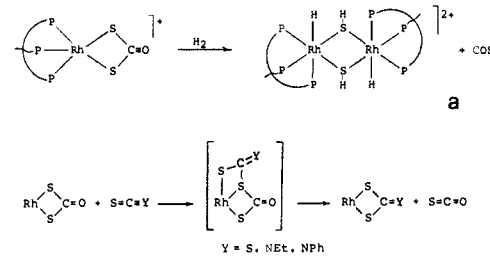

Scheme III

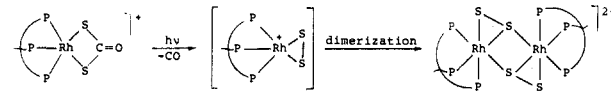

Scheme IV

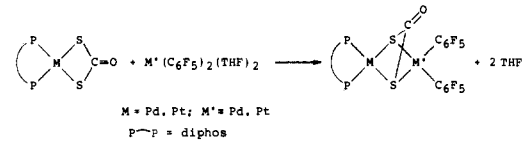

Scheme V

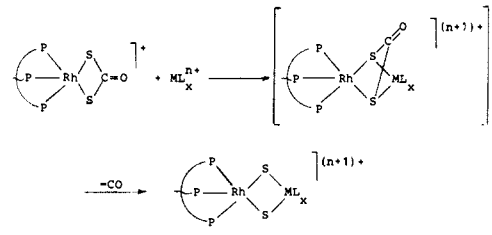

A somewhat different picture holds as far as the $[Rh/Fe]^+$ and $[Rh/Pt]^+$ dimers are concerned. Figure 7 shows the cyclic voltammogram exhibited by **4**. The i_{pa}/i_{pc} ratio of the first reduction step (E_p = −0.58 V), gradually increasing from 0.40 at 0.1 V s^{-1} to 0.80 at 10 V s^{-1}, clearly suggests that the electrogenerable species $[(triphos)Rh(\mu\text{-}S)_2Fe(CO)(etriphos)]$ is labile ($t_{1/2} \simeq 1$ s). Similarly, the absence of a response directly associated to the second reduction step (E_p = −1.42 V) even at the scan rate of 10 V s^{-1} indicates that the corresponding monoanion decomposes as soon as generated at the electrode surface. Also, the features of the most anodic responses in the reverse scan are consistent with the formation of transient intermediates during the decomposition of the primarily generated reduction species.

Finally, **3** displays a cyclic voltammetric response essentially similar to that of **4**, with a remarkable cathodic shift of the two reduction steps (E_p = −1.07 and −1.97 V, respectively, the latter being very close to the solvent discharge). Also in this case, the neutral species $[(triphos)Rh(\mu\text{-}S)_2Pt(diphos)]$ appears labile but with a lifetime some 10 times longer than that of **4**. In conclusion, both **3** and **4** are the only stable members of their potential redox chains.

Discussion

The chemistry of η^2-*S,S*-dithiocarbonate complexes of transition metals is highly influenced by the nucleophilic character of the sulfur atoms.[24,25] In addition to two nucleophilic sites of the latter type, the dithiocarbonate **5**, which is coordinatively and electronically unsaturated, contains an electrophilic metal center. Indeed, the dual nature of **5** makes it capable of cleaving H_2 in heterolytic fashion[26] (Scheme IIa) and metathesizing polarizable molecules such as the heteroallenes COS, CS_2, and SCNR (R

(18) Gagnē, R. R.; Spiro, C. L.; Smith, T. J.; Hamann, C. A.; Thies, W. R.; Shiemke, A. K. *J. Am. Chem. Soc.* **1981**, *103*, 4073.
(19) Gagnē, R. R.; Koval, C. A.; Smith, T. J. *J. Am. Chem. Soc.* **1977**, *99*, 8367.
(20) Gagnē, R. R.; Koval, C. A.; Smith, T. J.; Cimolino, M. C. *J. Am. Chem. Soc.* **1979**, *101*, 4571.
(21) Drago, R. S.; Desmond, M. J.; Corden, B. B. Miller, K. A. *J. Am. Chem. Soc.* **1983**, *105*, 2287.
(22) Robin, M. B.; Day, P. *Adv. Inorg. Chem. Radiochem.* **1967**, *10*, 247.
(23) Casewith, C. J.; Rakowski DuBois, M. *Inorg. Chem.* **1986**, *25*, 74.
(24) (a) Fackler, J. P., Jr.; Seidel, W. C. *Inorg. Chem.* **1969**, *8*, 1631. (b) Doherty, J.; Fortune, J.; Manning, A. R.; Stephens, F. S. *J. Chem. Soc., Dalton Trans.* **1984**, 1111.
(25) Bianchini, C.; Meli, A.; Vizza, F. *Angew. Chem., Int. Ed. Engl.* **1987**, *26*, 767.
(26) Bianchini, C.; Meli, A. *Inorg. Chem.* **1987**, *26*, 4268.

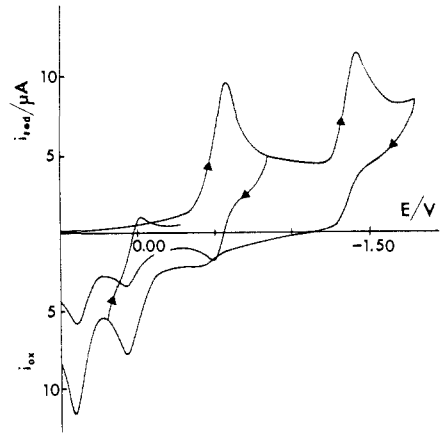

Figure 7. Cyclic voltammetric response recorded at a platinum electrode on a CH_2Cl_2 solution containing $[NBu_4]ClO_4$ (0.1 mol dm^{-3}) and $[(triphos)Rh(\mu\text{-}S)_2Fe(CO)(etriphos)]BPh_4$ (8.5×10^{-4} mol dm^{-3}). Scan rate 0.2 V s^{-1}.

Scheme VI

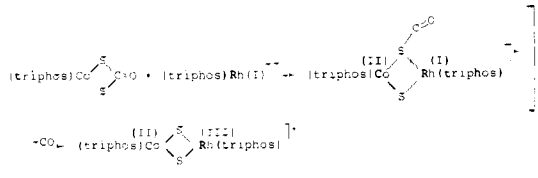

= Ph, Et) (Scheme IIb).[25] However, **5** possesses a third chemical property that, in conjunction with the nucleophilic character of the sulfur atoms, serves to understand the reactions described in Scheme I: compound **5** photochemically undergoes the chelotropic elimination of CO to form the bis(μ-η^2-disulfur) complex $[(triphos)Rh(\mu\text{-}S_2)_2Rh(triphos)]^{2+}$ (Scheme III).[27]

On the basis of the known chemistry of **5** as well as the recently reported synthesis of a family of μ-η^2-*S*,*S*-dithiocarbonate dimers via reaction of η^2-*S*,*S*-dithiocarbonate mononuclear complexes with coordinatively unsaturated metal fragments (Scheme IV)[28] a reasonable mechanism to explain the facile formation of the present bis(μ-sulfido) dimers is the one shown in Scheme V. This involves interaction between $[(triphos)Rh(S_2CO)]^+$ and the coordinatively unsaturated ML_x^{n+} fragments via the two sulfur atoms of the dithiocarbonate ligand. As a result, the S–C bonds are cleaved, and the carbonyl group is chelotropically eliminated as free (Rh, Pt, Co) or complexed (Fe) carbon monoxide. Since the formal oxidation state of the entering metals in the final products is generally raised by 2, one can reasonably assume that electrons are transferred from the ML_x^{n+} fragments into strongly antibonding C–S orbitals of the rhodium dithiocarbonate system. The presence of a low-energy antibonding MO centered on the C–S linkages in **5** has been ascertained experimentally[27] and confirmed theoretically.[29]

A mechanism of the type shown in Scheme V fully rationalizes the final formal oxidation states of the metals in the $[Rh/Rh]^{2+}$ and $[Rh/Pt]^+$ dimers as well as in the $[Rh/Co]^+$ complex, which reasonably forms through an identical path (Scheme VI).

The diverging behavior of the cobalt and iron reactions (the oxidation state of cobalt is raised by one only whereas that of iron remains unchanged) is interpreted in terms of redox chemistry: The expected products ($[Rh/Co]^{3+}$ and $[Rh/Fe]^{3+}$, respectively) would be extremely poor in electrons and, hence, easily reducible. In this respect, notice that the environment of the reactions is a very reducing one owing to the presence of tertiary phosphines, BPh_4^- anions, and ethanol.[8] Chemical and electrochemical attempts have been made to try to oxidize compounds **2** and **4** in several aprotic solvents: Despite color changes occurring on oxidation, in no case was a stable product obtained, the starting complexes being invariably collected after the addition of ethanol.

As a final mechanistic consideration, the reaction of **5** with the $(triphos)Ni^{2+}$ fragment, although leading to an unexpected dinickel μ-S species, supports the hypothesis that the sulfur atoms of the dithiocarbonate ligand are indeed the sites attacked by the externally added electrophilic metal fragments. In this respect, it is worth noting that both μ-sulfido groups[2h] and S atoms belonging to η^2-*S*,*S*-dithiocarbamate ligands[30] still exhibit nucleophilic character and can coordinate metal systems.

Reactions of the Bis(μ-sulfido) Complexes with H_2. All of the bis(μ-sulfido) compounds here described have been reacted with dihydrogen [298 K (1 atm)]. With the exception of the $[Rh/Rh]^{2+}$ dimer (see eq 1), in no case was a chemical transformation observed, even for very long reaction times. This is a clear indication that, besides the right choice of the metals, a precise electronic configuration is requested to design a compound capable of activating molecular hydrogen: Notice, in fact, that the addition of one or two electrons to **1** fully deletes the reactivity toward H_2!

When semiempirical MO methods are used, the interaction between two H_2 molecules and the Rh_2S_2 framework in **1** has been investigated recently.[31] The calculations indicate that the double hydrogenation of **1** is technically feasible on account of a strongly avoided crossing between isosymmetric HOMO–LUMO levels. Also, of particular relevance for the reaction with H_2 appears the distribution of four electrons over the π system of the Rh_2S_2 planar ring in **1**.[32] A situation is observed for other rhodium(III) complexes containing planar tetraatomic RhSSC(X) rings (X = O, S, NR) and capable of heterolytically splitting H_2.[26]

Experimental Section

General Procedure. All the reactions and manipulations were routinely performed under a nitrogen or argon atmosphere by standard Schlenk techniques. In order to prevent photochemical decomposition, the reactions involving the dithiocarbonate **5** were carried out in near-darkness. The compounds $[(triphosRh(S_2CO)]BPh_4$,[7] $(triphos)Co(S_2CO)$,[13] $[(C_2H_4)_2RhCl]_2$,[33] and $(PPh_3)_2Pt(C_2H_4)$[34] and the ligands triphos[35] and etriphos[9] were prepared according to published procedures. The ligand diphos was purchased from Strem Chemicals and used without further purification. Solvents and other chemicals were all of reagent-grade quality and, unless otherwise stated, were used as received from the commercial suppliers. Tetrahydrofuran (THF) was purified by distillation under nitrogen over $LiAlH_4$ just before use. The solid compounds were routinely collected on sintered-glass frits and washed successively with ethanol and petroleum ether before being dried in a nitrogen stream.

Analytical Instrumentation. Carbon monoxide evolution during the reaction was detected by GC on a Carbosieve S-II column (Supelco). Infrared spectra were recorded on a Perkin-Elmer 283 spectrophotometer with samples mulled in Nujol between KBr plates. $^{31}P\{^1H\}$ NMR spectra were recorded on Varian CFT 20 and VXR 300 spectrometers operating at 32.19 and 121.42 MHz, respectively. Peak positions are relative to H_3PO_4 (85%) with downfield values reported as positive. Conductance measurements were made with a WTW Model LBR/B conductivity bridge. Ultraviolet–visible spectra were recorded on a Beckman DK-2A spectrophotometer. Magnetic susceptibilities of solid samples were measured on a Faraday balance. The materials and the apparatus used for the electrochemical experiments have been described elsewhere.[10] The potential values are relative to an aqueous calomel electrode (SCE). The temperature was controlled at 20 ± 0.1 °C. Under the present experimental conditions, the ferrocenium/ferrocene couple was located at +0.38 V. X-Band EPR spectra were recorded with an ER 200-SRCB Bruker spectrometer operating at w_0 = 9.78 GHz. The control of the external magnetic field was obtained with a microwave-bridge ER 041 MR Bruker wave meter. The temperature was varied and controlled with an ER 4111 VT Bruker device with an accuracy of ±1 K. In order to estimate accurate g_{iso} and g_{aniso} values over the temperature range of interest, the diphenylpicrylhydrazyl (DPPH) free radical was used as field marker (g_{iso} (DPPH) = 2.0036, w_0 = 9.43 GHz). In order to ensure

(27) Bianchini, C.; Meli, A. *Inorg. Chem.* **1987**, *26*, 1346.
(28) Fornies, J.; Uson, M. A.; Gil, J. I.; Jones, P. *J. Organomet. Chem.* **1986**, *311*, 243.
(29) We thank Dr. C. Mealli, ISSECC, CNR, for this result.
(30) McCleverty, J. A.; McLuckie, S.; Morrison, N. J.; Bailey, N. A.; Walker, N. W. *J. Chem. Soc., Dalton Trans.* **1977**, 359.
(31) Mealli, C.; Bianchini, C., submitted for publication.
(32) Bianchini, C.; Mealli, C.; Meli, A.; Sabat, M. *Abstracts of Papers*, XIX Congresso Nazionale di Chimica Inorganica, Santa Margherita di Pula, Cagliari, Italy, Oct 1986; A34.
(33) Cramer, R. *Inorg. Synth.* **1974**, *15*, 14.
(34) Nagel, U. *Chem. Ber.* **1982**, *115*, 1998.
(35) Hewertson, W.; Watson, H. R. *J. Chem. Soc.* **1962**, 1940.

quantitative reproducibility, the samples were placed into calibrated quartz capillary tubes permanently positioned in the resonance cavity.

[(Triphos)Rh(μ-S)$_2$Rh(triphos)](BPh$_4$)$_2$ (1). A mixture of [(C$_2$H$_4$)$_2$RhCl]$_2$ (0.07 g, 0.18 mmol) and AgBF$_4$ (0.07 g, 0.36 mmol) in THF (30 mL) was stirred for 1 h. After elimination of the precipitated AgCl, the filtrate was treated first with solid triphos (0.22 g, 0.36 mmol) and then with [(triphos)Rh(S$_2$CO)]BPh$_4$ (0.40 g, 0.35 mmol) in CH$_2$Cl$_2$ (20 mL). An immediate reaction occurred accompanied by carbon monoxide evolution. Brown crystals were formed following the addition of NaBPh$_4$ (0.14 g, 0.4 mmol) in ethanol (30 mL) and the slow evaporation of the solvent: yield 72%; Λ_M 103 cm^2 Ω^{-1} mol^{-1}. Anal. Calcd for C$_{130}$H$_{118}$B$_2$P$_6$Rh$_2$S$_2$: C, 72.36; H, 5.51; Rh, 9.53; S, 2.97. Found: C, 72.01; H, 5.65; Rh, 9.38; S, 2.83.

[(Triphos)Rh(μ-S)$_2$Co(triphos)](BPh$_4$)$_2$ (2). To azeotrope off the water of the perchlorate salt, a solution of Co(ClO$_4$)$_2$·6H$_2$O (0.13 g, 0.35 mmol) in *n*-butanol (100 mL) was gently concentrated by heating at boiling temperature to ca. 5 mL. Triphos (0.22 g, 0.35 mmol) in CH$_2$Cl$_2$ (10 mL) was then added. The resulting light orange solution was treated with [(triphos)Rh(S$_2$CO)]BPh$_4$ (0.4 g, 0.35 mmol) in CH$_2$Cl$_2$ (20 mL). As above carbon monoxide evolved. Addition of NaBPh$_4$ (0.14 g, 0.4 mmol) in ethanol (30 mL) and partial evaporation of the solvent under a slow stream of nitrogen gave brown crystals: yield 60%; Λ_M 98 cm^2 Ω^{-1} mol^{-1}. Anal. Calcd for C$_{130}$H$_{118}$B$_2$CoP$_6$RhS$_2$: C, 73.86; H, 5.62; Co, 2.78; Rh, 4.86; S, 3.03. Found: C, 73.21; H, 5.55; Co, 2.69; Rh, 4.77; S, 2.94. *Caution!* To avoid detonation of Co(ClO$_4$)$_2$, the solution must not be taken to near-dryness and solid material must not be allowed to deposit on the walls of the reaction flask. It is recommended that one work behind a protective barrier.

[(Triphos)Rh(μ-S)$_2$Pt(diphos)]BPh$_4$ (3). A solution of [(triphos)Rh(S$_2$CO)]BPh$_4$ (0.40 g, 0.35 mmol) in THF (20 mL) was added to a solution of (PPh$_3$)$_2$Pt(C$_2$H$_4$) (0.26 g, 0.35 mmol) in THF (10 mL). Immediately the color turned to deep red, and carbon monoxide evolved. Solid diphos (0.14 g, 0.35 mmol) was then added to the mixture, which was stirred for 15 min. Addition of NaBPh$_4$ (0.14 g, 0.4 mmol) in ethanol (30 mL) led to the precipitation of red crystals: 68%; Λ_M 41 cm^2 Ω^{-1} mol^{-1}. Anal. Calcd for C$_{91}$H$_{83}$BP$_5$PtRhS$_2$: C, 64.12; H, 4.90; Pt, 11.44; Rh, 6.03; S, 3.76. Found: C, 64.01; H, 4.85; Pt, 11.33; Rh, 5.98; S, 3.66.

[(Triphos)Rh(μ-S)$_2$Fe(CO)(etriphos)]BPh$_4$ (4). A solution of [(triphos)Rh(S$_2$CO)]BPh$_4$ (0.40 g, 0.35 mmol) in CH$_2$Cl$_2$ (20 mL) was added to a mixture of Fe(BF$_4$)$_2$·6H$_2$O (0.12 g, 0.35 mmol) in ethanol (10 mL) and etriphos (0.12 g, 0.35 mmol) in CH$_2$Cl$_2$ (20 mL) to give immediately a deep violet color. When the resulting solution was gently heated at 35 °C for 20 min, the color turned deep green. Upon addition of NaBPh$_4$ (0.14 g, 0.4 mmol) in ethanol (30 mL), green crystals were obtained: 73%; Λ_M 45 cm^2 Ω^{-1} mol^{-1}. Anal. Calcd for C$_{83}$H$_{98}$BFeOP$_6$RhS$_2$: C, 65.10; H, 6.45; Fe, 3.64; Rh, 6.72; S, 4.18. Found: C, 64.99; H, 6.41; Fe, 3.33; Rh, 6.58; S, 4.06.

[(Triphos)Rh(μ-S)$_2$Co(triphos)]BPh$_4$ (7). Method A. A mixture of [(C$_2$H$_4$)$_2$RhCl]$_2$ (0.07 g, 0.18 mmol) and AgBF$_4$ (0.07 g, 0.36 mmol) in THF (30 mL) was stirred for 1 h. After elimination of the precipitated AgCl, the filtrate was first treated with solid triphos (0.22 g, 0.36 mmol) and then with (triphos)Co(S$_2$CO) (0.27 g, 0.35 mmol) in CH$_2$Cl$_2$ (20 mL). An immediate reaction occurred accompanied by carbon monoxide evolution. Brown crystals were formed following the addition of NaBPh$_4$ (0.14 g, 0.4 mmol) in ethanol (30 mL) and the slow evaporation of the solvent; yield 62%.

Method B. NaBH$_4$ (10 mg, 0.26 mmol) in ethanol (10 mL) was added dropwise to a solution of **2** (0.32 g, 0.15 mmol) in CH$_2$Cl$_2$ (25 mL), which turned from orange-brown to red. Addition of ethanol (30 mL) and partial evaporation of the solvent under a fast stream of nitrogen gave red crystals: 35%; Λ_M 43 cm^2 Ω^{-1} mol^{-1}. Anal. Calcd for C$_{106}$H$_{98}$BCoP$_6$RhS$_2$: C, 70.94; H, 5.50; Co, 3.28; Rh, 5.73; S, 3.57. Found: C, 70.01; H, 5.55; Co, 3.27; Rh, 5.68; S, 3.43.

[(Triphos)Rh(μ-S)$_2$Rh(triphos)]BPh$_4$ (8). Method B reported above for **7** was successfully used for the preparation of this red compound except for substitution of **1** for **2**: yield 49%; Λ_M 45 cm^2 Ω^{-1} mol^{-1}. Anal. Calcd for C$_{106}$H$_{98}$BP$_6$Rh$_2$S$_2$: C, 69.24; H, 5.37; Rh, 11.19; S, 3.48. Found: C, 69.31; H, 5.24; Rh, 11.06; S, 3.43.

[(Triphos)Ni(μ-S)Ni(triphos)](BPh$_4$)$_2$ (9). A solution of [(triphos)Rh(S$_2$CO)]BPh$_4$ (0.40 g, 0.35 mmol) in CH$_2$Cl$_2$ (20 mL) was added to a mixture of Ni(BF$_4$)$_2$·6H$_2$O (0.12 g, 0.35 mmol) in ethanol (15 mL) and triphos (0.22 g, 0.35 mmol) in CH$_2$Cl$_2$ (20 mL). An immediate reaction occurred accompanied by carbon monoxide evolution. After the solution stood for 3 h, the originally formed dark brown color turned deep green. Green crystals were formed following the addition of NaBPh$_4$ (0.14 g, 0.4 mmol) in ethanol (30 mL) and the slow evaporation of the solvent; yield 15%.

Registry No. 1, 105139-43-3; **2**, 113686-46-7; **3**, 113686-48-9; **4**, 113686-50-3; **5**, 99955-64-3; **6**, 82590-72-5; **7**, 113686-52-5; **8**, 113686-54-7; **9**, 58593-52-5; (PPh$_3$)$_2$Pt(C$_2$H$_4$), 12120-15-9; [(C$_2$H$_4$)$_2$RhCl]$_2$, 12081-16-2; [(triphos)Co(μ-S)$_2$Co(triphos)]$^{2+}$, 73496-95-4; [(triphos)Co(μ-S)$_2$Co(triphos)]$^+$, 113686-57-0; [(triphos)Co(μ-S)$_2$Co(triphos)], 73770-23-7; [(triphos)Co(μ-S)$_2$Rh(triphos)], 113686-56-9; [(triphos)Rh(μ-S)$_2$Rh(triphos)], 113686-55-8; dithiocarbonic acid, 4741-30-4.

New Crystalline Phase of (Octaethylporphinato)nickel(II). Effects of π-π Interactions on Molecular Structure and Resonance Raman Spectra

Theodore D. Brennan,[1] W. Robert Scheidt,*[1] and John A. Shelnutt*[2]

Contribution from the Department of Chemistry, University of Notre Dame, Notre Dame, Indiana 46556, and Fuel Sciences Division, Sandia National Laboratories, Albuquerque, New Mexico 87185. *Received October 19, 1987*

Abstract: A new (third) crystalline phase of Ni(OEP) has been isolated and characterized by a single-crystal X-ray diffraction study and single-crystal resonance Raman spectroscopy. Single-crystal Raman measurements were also performed on the two previously described phases and the Raman spectra of the three phases compared. Differences in Raman spectra between the current new phase and the previously reported triclinic phase are interpreted in terms of π-π interactions found for this new phase. These spectral differences are also compared to solution Raman data that had been previously reported on aggregated and monomeric porphyrin derivatives. The bands most affected are the core-size marker bands ν_{10}, ν_{19}, and ν_3 and the oxidation-state marker band ν_4 where π-π interaction leads to increases of 2.5-4.3 cm^{-1}. These Raman shifts are consistent with a decrease in the core size, and the crystal structure confirms this interpretation. The two crystallographically distinct Ni-N bond distances in the new crystalline phase are 1.946 (4) and 1.958 (4) Å, with the shorter distance along the one-dimensional stack axis of the complex. The observed interplanar spacing between porphyrin planes is 3.44 Å, and the Ni···Ni separation is 4.80 Å. Crystal data: triclinic; space group $P\bar{1}$; a = 13.302 (6), b = 13.342 (11), c = 4.802 (2) Å; α = 92.21 (2), β = 93.52 (4), γ = 113.43 (6)°; Z = 1; V = 778.7 Å^3. A total of 2568 unique observed data to a maximum (sin θ)/λ of 0.726 was used in the structure solution and refinement.

Meyer[3] and Cullen and Meyer[4] have reported the crystal and molecular structure of two different crystalline phases of four-coordinate (2,3,7,8,11,12,17,18-octaethylporphinato)nickel(II), Ni(OEP).[5] An important feature of these two crystalline phases

0002-7863/88/1510-3919$01.50/0